Malaysian Journal of Chemistry, 2026, Vol. 28(2), 163-179

Characterization of Polysaccharide Blend Films for Potential Polymer Hosts in Polymer Electrolytes

Farihah Jaafar[1], Effa Arisya Suhaimi[1], Nabilah Akemal Muhd Zailani[1]*, Khuzaimah Nazir[1] and Pramodh K. Singh[2]

[1]Faculty of Applied Sciences, Universiti Teknologi MARA, Kampus Arau, 02600 Arau, Perlis, Malaysia
[2]COE on Solar Cells and Renewable Energy, School of Basic Sciences and Research, Sharda University, Greater Noida, 201310, India
*Corresponding author (email: nabilahakemal@uitm.edu.my)

This study aims to develop a superior polymer electrolyte by blending natural polymers, tamarind seed polysaccharide (TSP) and pectin, with carrageenan to overcome the issue of film brittleness caused by hydrogen bonding. Using solvent casting technique, TSP and pectin with different ratios of carrageenan (0:100, 20:80, 40:60, 60:40, 80:20, and 100:0) were prepared. This work successfully produced flexible, free-standing TSP/carrageenan and pectin/carrageenan blend films at an optimal 40:60 ratio which showed increased tensile strain and improved flexibility, demonstrating the synergistic effect. This is attributed to the interaction between the blended polymers, as confirmed by FTIR analysis, which inhibits the formation of hydrogen bonds. The improved flexibility also contributes to enhanced ionic conductivity. Incorporating 15 wt% of lithium triflate (LiTf) salt into the pectin/carrageenan blend system boosted ionic conductivity by one order of magnitude, from 6.58×10^{-7} S cm^{-1} to 2.95×10^{-6} S cm^{-1}. This enhancement is due to the presence of conducting species from the salt and the creation of new ion pathways, as confirmed by the optical micrograph.

Keywords: Polymer blend, polymer electrolytes, pectin, tamarind seed polysaccharide, carrageenan.

Received: July 2025; Accepted: December 2025

Liquid electrolytes have been traditionally used in electrochemical products such as batteries due to their high ionic conductivity. Nevertheless, since it is in liquid form, there is a chance that it will leak and cause possible danger. Also, other disadvantages of liquid electrolytes include poor ion selectivity and electrochemical instability [1]. Due to these issues, polymer electrolytes (PEs) have been chosen as an alternative for liquid electrolytes. PEs, which are frequently found in lithium-ion batteries, are made up of polymers and ionic salts [1]. PEs offer inherent safety, greater electrochemical and thermal stability, and are lightweight [2]. Polymer host can originate from natural polymers or synthetic polymers. Natural polymers are primarily derived from plant and animal sources, such as polysaccharides, proteins, and polyesters, whereas synthetic polymers are artificially created, such as polyethylene (PE) and poly(methyl methacrylate) (PMMA) [3]. The environmental friendliness of natural polymer electrolytes has therefore piqued interest in more research.

Pectin and tamarind seed polysaccharide (TSP) are naturally occurring polymer from plants. However, pectin and TSP films exhibit brittleness which will limit the ionic conductivity of the PE system. The brittle electrolyte films will cause poor electrode-electrolyte adhesion and lower the ionic conductivity of the system, which will affect its performance in energy storage devices applications. The brittleness of the films is due to the presence of OH groups which are susceptible to physical crosslinking via hydrogen bonding. There are some alternatives to improve the brittleness and ionic conductivity of the system, such as by adding plasticizers and fillers and polymer blending. Ethylene carbonate (EC), propylene carbonate (PC), phthalates, and bisphenols are examples of plasticizers [4]. A previous study, however, reports that the exposure of plasticizers such as phthalates and bisphenols might pose a danger to humans [5]. Qadeer et al. [6] further reported that phtalate plasticizer may have toxicity. Meanwhile, the addition of fillers also could increase ionic conductivity; however, adding excessive amounts of nanofillers will cause agglomeration on the PE films [7]. Therefore, polymer blending is more preferred to overcome the brittleness issues of pectin and TSP films. Polymer blend can be defined as a mixture of two or more polymers [8].

In this study, carrageenan has been proposed to be blended with pectin and TSP. This is due to its exceptional features, which include flexibility, biocompatibility, and moldability which may be projected to overcome the brittleness of pectin films [9]. Thus, in this study, the structural, morphological,

mechanical, and electrical properties of the pectin/ carrageenan and TSP/carrageenan blend films of different ratios were investigated using Fourier transform infrared (FTIR) spectroscopy, optical microscopy (OM), universal testing machine (UTM), and electrochemical impedance spectroscopy (EIS), respectively.

Previously, pectin had been blended with sodium alginate, and the highest ionic conductivity of 1.26×10^{-7} S cm^{-1} was recorded at 303 K [10]. Meanwhile, Perumal et al. [11] reported that TSP with 0.3 (m.m.%) of magnesium perchlorate ($Mg(ClO_4)_2$ shows the ionic conductivity value of 5.18×10^{-7} S cm^{-1}. The value obtained are low if compared to the minimum value of ionic conductivity for the energy storage application (~10^{-3} S cm^{-1}). Therefore, lithium triflate (LiTf) was added into the best blend composition to provide the conducting species and enhance the ionic conductivity of the system. The structural, morphological, and electrical properties of the LiTf-doped polymer blend film were studied using FTIR, OM, and EIS, respectively.

EXPERIMENTAL

Chemicals and Materials

Pectin (Galacturonic acid ≥ 74.0 %) and LiTf (Purity: 99.995 %) were obtained from Merck (Darmstadt, Germany), while TSP and carrageenan were purchased from Tokyo Chemical Industry, Japan, and Sigma-Aldrich, respectively.

Preparation of the Polymer Blend Films

The film samples of pectin/carrageenan and TSP/ carrageenan were prepared by using the solution casting technique modified from the study by Habep et al. [12]. In accordance with **Table 1**, TSP and carrageenan were dissolved in distilled water by vigorous stirring at 80ºC and 50ºC, respectively, before mixing. The mixture was cast onto a petri dish and allowed to dry in the oven for 24 hours, or until a film formed at the temperature of 60°C. The polymer blend film was then subjected to characterization.

Preparation of the Salt-doped Polymer Blend Film

The best composition of the polymer blends was doped with 15 wt% LiTf. 0.3529 g of LiTf salt was added into the polymer blend mixture and thoroughly dissolved by continuously stirring for an hour. 15 wt% of salt was chosen to dope the optimum ratio polymer blend because it is within the wt% range of salt that exhibits the highest ionic conductivity when it is incorporated into the blend system [13,14]. The mixture was then poured into a petri dish and left in an oven for drying to generate films. The film was kept in the desiccator before further characterization.

Characterization Methods

Fourier Transform Infrared Spectroscopy (FTIR)

Interactions between constituents in the polymer blends were investigated using FTIR (Thermo Fischer Scientific Nicolet iS 10) with Attenuated Total Reflectance (ATR). The films were placed onto the crystal and observations were done in the frequency range of 4000 – 600 cm^{-1} at 2 cm^{-1} resolution and 16 scans.

Optical Microscopy (OM)

Optical Microscopy (Olympus) was used to observe the morphology of the polymer blend films. The samples were observed at 10× magnification.

Universal Tensile Machine (UTM)

Tensile strength was measured with the Instron Universal Testing Instrument (3365, Instron USA), which is made up of tensile stress (MPa), Young's modulus (MPa), and tensile strain (%). The sample from each film was cut into 1.0 cm × 5.0 cm pieces, in accordance with ASTM D882, and a cross-speed of 5 mm/min was employed. Each measurement of the samples was performed three times.

Table 1. The composition of polymer blend films.

Ratio pectin or TSP:carrageenan	Mass of pectin or TSP (g)	Mass of carrageenan (g)	Designations (pectin:carrageenan system)	Designation (TSP:carrageenan system)
100:0	2.0000	0.0000	Pectin	TSP
20:80	0.4000	1.6000	PE20	TSP20
40:60	0.8000	1.2000	PE40	TSP40
60:40	1.2000	0.8000	PE60	TSP60
80:20	1.6000	0.4000	PE80	TSP80
0:100	0.0000	2.0000	Carrageenan	Carrageenan

Electrochemical Impedance Spectroscopy (EIS)

The method used to determine the ionic conductivity of the polymer blend electrolyte was EIS (HIOKI 35232-01 LCR). The electrolyte films were tested at room temperature in the frequency range of 100 Hz to 1 MHz. Impedance was measured after polymer electrolyte films were positioned between the two blocking electrodes made of stainless steel. The thickness of the electrolyte films was measured using a micrometre screw gauge before the measurement. Impedance was measured on three different parts of each film and the mean ionic conductivity for each sample was considered using Equation (1).

$$\sigma = L/(A.R_b) \quad (1)$$

All measurements were conducted in triplicate, and the data are reported as mean ± standard deviation to ensure data reliability and reproducibility. While X-ray diffraction (XRD) and differential scanning calorimetry (DSC) are excellent for directly determining structural properties like amorphosity, they were not conducted due to certain limitations. Nevertheless, the comprehensive analyses from FTIR, UTM, and EIS provided sufficient evidence to justify the material's amorphous properties.

RESULTS AND DISCUSSION

Formation of Polymer Blend Films

The pure TSP, pure carrageenan and pure pectin films were brittle (**Figures 1(a)**, **(b)**, and **(g)**), with visible cracks and fractures. This might be due to the formation of hydrogen bonding between the individual polymer chains. The same observations were reported by Butler et al. [15] and Fauzee et al. [16] for pure pectin and TSP films, respectively.

The blend film of TSP/carrageenan at a ratio of 20:80 was slightly brittle and showed phase separation, as shown in **Figure 1(c)**. This might be due to the incompatibility of both polymers at that ratio. As the amount of TSP increased, the films became homogenous and flexible, as shown in **Figures 1(d)-(f)** for TSP/carrageenan with the ratios of (40:60), (60:40), (80:20), respectively. Meanwhile, for the pectin/carrageenan system, PE20, PE60 and PE80 were totally brittle (**Figures 1(h)**, **(j)**, and **(k)**), and the flexible film was only observed for PE40. From the results, the best ratio to get the flexible film is 40:60 of pectin/carrageenan. This is supported by the study by Said et al. [17], which states that only a moderate quantity of pectin in a pectin/PLA blend will strengthen the film.

Structural Studies of Polymer Blend Films

With the aim of confirming the chemical structure of the polymer blend films, FTIR analyses were conducted. **Figure 2** illustrates the FTIR spectra of TSP/carrageenan-blend films. Meanwhile, **Table 2** lists FTIR peaks for the system. The peaks for pure TSP appeared at 3310 cm^{-1}, 2895 cm^{-1}, 1643 cm^{-1}, and 1008 cm^{-1}, representing O–H stretching, C–H stretching, C=C stretching, and C–O–C stretching, respectively. The same FTIR peaks of TSP had been observed, as reported by Fauzee et al. [16].

The peaks for carrageenan appeared at 3363 cm^{-1}, 2909 cm^{-1}, 1634 cm^{-1}, 1225 cm^{-1}, 1032 cm^{-1}, and 844 cm^{-1}, representing O–H stretching, C–H stretching, C=C stretching, S=O stretching, C–O–C stretching, and O–SO_3 stretching, respectively. The same FTIR peaks of carrageenan were observed and reported by Serra et al. [18] and Alshammari et al. [19]. Following blending with TSP, the FTIR spectrum showed the S=O stretching and O–SO_3 stretching peaks which correspond to the sulfate ester of carrageenan, indicating that the blending between the two components was successful.

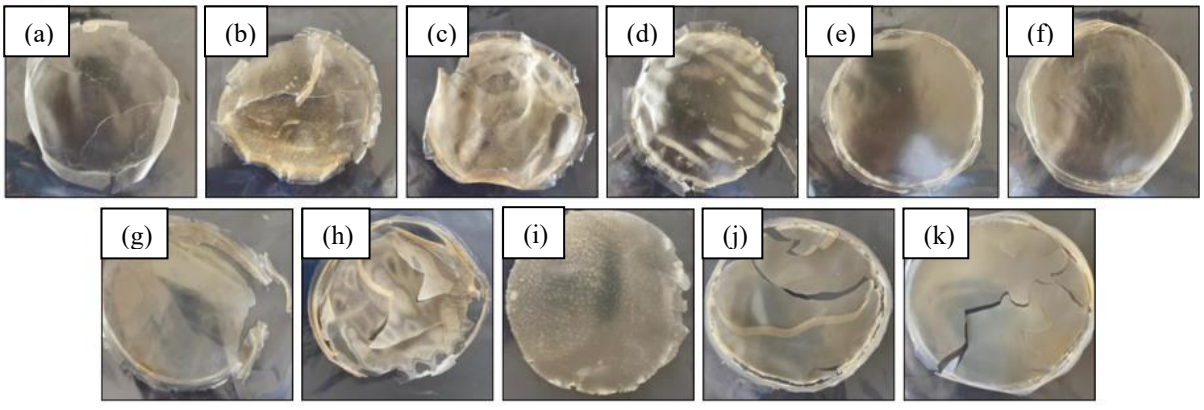

Figure 1. Films of (a) pure TSP, (b) carrageenan, (c) TSP 20, (d) TSP 40, (e) TSP 60, (f) TSP 80, (g) pure pectin, (h) PE20, (i) PE40, (j) PE60, and (k) PE80.

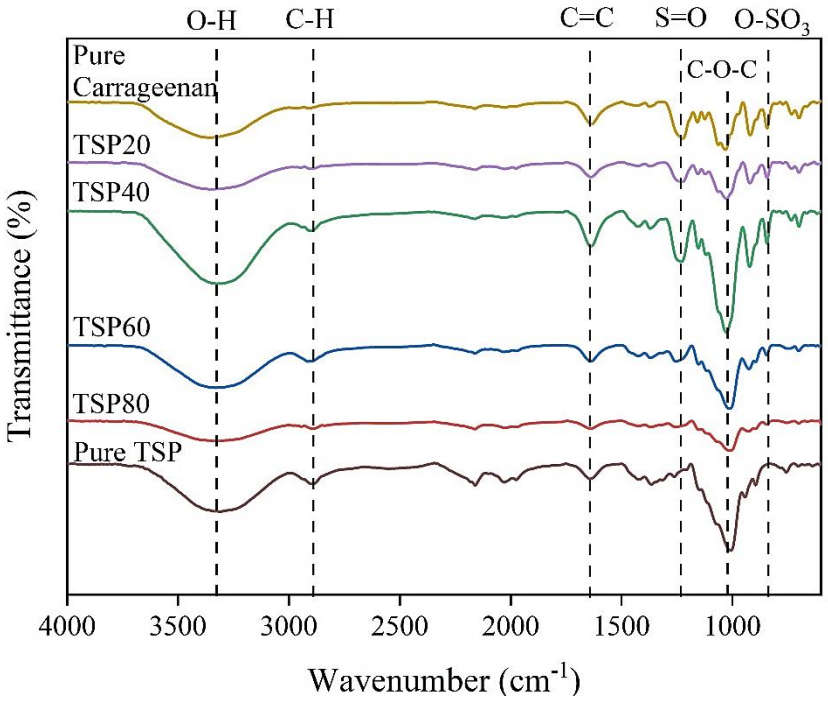

Figure 2. FTIR spectra of the TSP/carrageenan polymer blend films.

Table 2. List of FTIR peaks for TSP/carrageenan films.

Wavenumber (cm^{-1})						Peak Assignment
Pure TSP	TSP20	TSP40	TSP60	TSP80	Carrageenan	
3310	3358	3325	3329	3319	3363	O-H stretching
2895	2900	2892	2912	2892	2909	C-H stretching
1643	1640	1638	1641	1645	1634	C=C Stretching
-	1229	1231	1254	1250	1225	S=O stretching
1008	1026	1026	1016	1013	1032	C-O-C stretching
-	844	844	845	845	844	$-O-SO_3$ stretching

The O–H stretching peak of TSP shifted to higher wavenumbers, from 3310 cm^{-1} to 3358, 3325, 3329, and 3319 cm^{-1}, respectively, for different ratios of TSP/carrageenan blends (TSP20, TSP40, TSP60, TSP80). The peak that represents the C=C stretching shifted from 1643 cm^{-1} of pure TSP to 1640, 1638, 1641, and 1645 cm^{-1}, respectively. The peak at 1008 cm^{-1}, which corresponds to the C–O–C stretching of pure TSP, shifted to 1026, 1026, 1016, and 1013 cm^{-1}, respectively, with decrease in intensity at different compositions of TSP/carrageenan. Hence, the peak shifting and intensity changes seen in the TSP/ carrageenan blend system indicate that the hydrogen bonding interaction happened between the polymers.

Figure 3 illustrates the FTIR spectra of the pectin/carrageenan polymer blend films, while **Table 3** lists FTIR peaks for the system. The peaks for pectin appeared at 3284, 2917, 1735, and 1014 cm^{-1}, representing O–H stretching, C–H stretching, C=O stretching, and C–O–C stretching, respectively. The same observation was reported by Halim et al. [20].

After polymer blending, the appearance of S=O stretching and O–SO_3 stretching peaks representing carrageenan indicates the successful blending. The O–H stretching peak shifted to higher wavenumbers, from 3284 cm^{-1} for pure pectin to 3362, 3327, 3319, and 3307 cm^{-1} for PE20, PE40, PE60, and PE80, respectively. Meanwhile, for the C=O stretching, it shifted from 1735 cm^{-1} for pure pectin to 1736, 1744, 1747, and 1738 cm^{-1} for PE20, PE40, PE60, and PE80, respectively. The C–H stretching peak shifted to higher wavenumbers, from 2917 cm^{-1} for pure pectin to 2945, 2971, 2943, and 2948 for PE20, PE40, PE60, and PE80, respectively. Thus, the changes in wavenumber for all these peaks indicate the occurrence of hydrogen bonding interaction between pectin and carrageenan chain. The hydrogen bonding interaction between the polymers was also reported by the studies done by Zainuddin et al. [21] and Liu et al. [22] on the polymer blend of CMC/kappa-carrageenan.

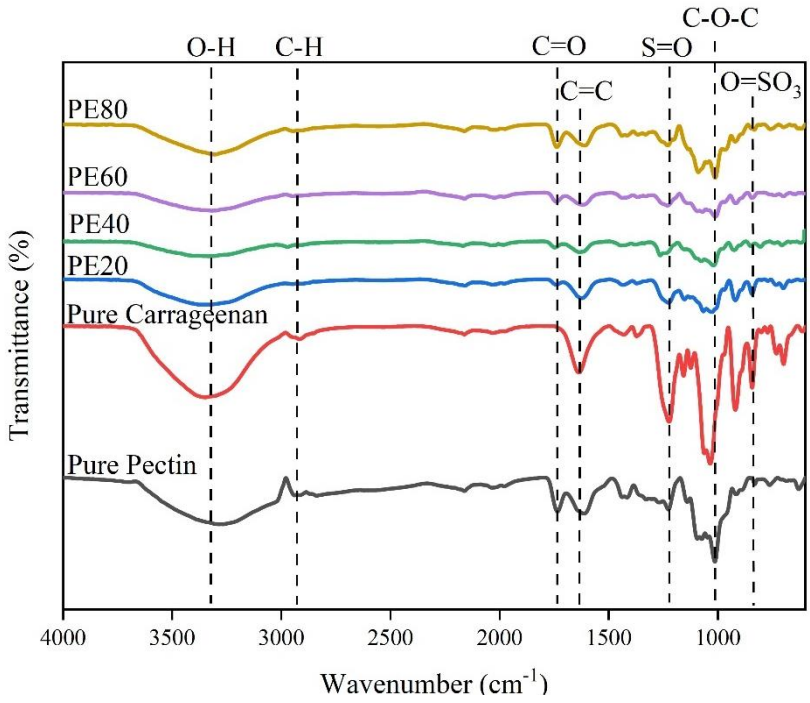

Figure 3. FTIR spectra of the pectin/carrageenan polymer blend films.

Table 3. List of FTIR peaks for pectin/carrageenan films.

Wavenumber (cm^{-1})						Peak Assignment
Pure Pectin	PE20	PE40	PE60	PE80	Carrageenan	
3284	3362	3327	3319	3307	3349	O-H stretching
2917	2945	2971	2943	2948	2917	C-H stretching
1735	1736	1744	1747	1738	-	C=O Stretching
-	1226	1257	1231	1230	1224	SO_3 stretching
1014	1027	1013	1011	1013	1036	C-O-C stretching

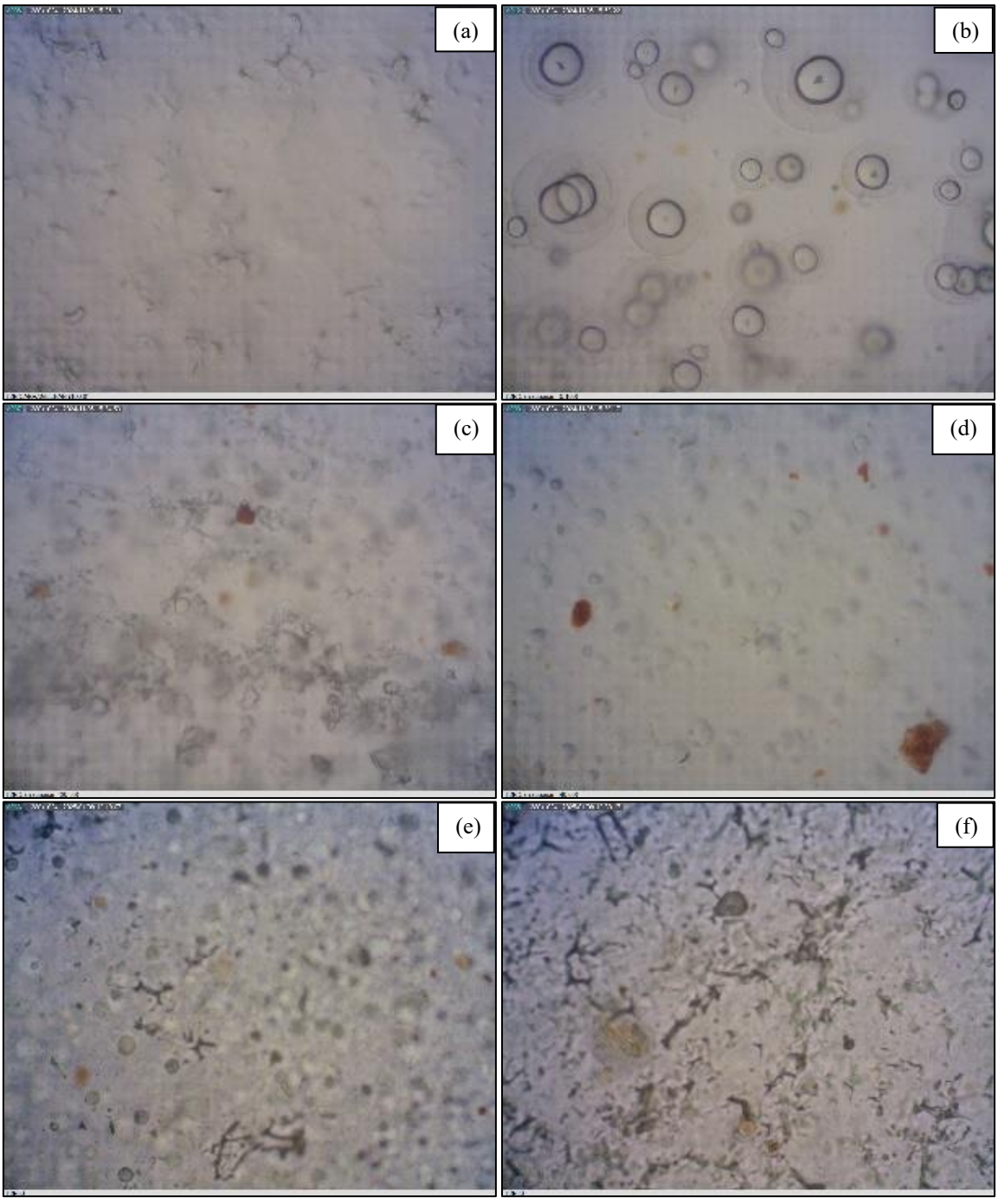

Figure 4. Optical micrographs of (a) pure TSP, (b) carrageenan, (c) TSP20, (d) TSP40, (e) TSP60, and (f) TSP80.

Morphological Studies of Polymer Blend Films

Figure 4 presents the optical micrographs of pure TSP, pure carrageenan, and different ratio TSP/ carrageenan polymer blend films (TSP20, TSP40, TSP60, TSP80). The morphology of pure TSP showed a uniform surface morphology but with visible wrinkles and folds that indicate the film exhibits brittleness, which can lead to crack initiation (**Figure 4(a)**). **Figure 4(b)** shows that the surface of pure carrageenan had a more textured surface with obvious microstructures. This can be correlated with the observation by Sudhakar et al. [23] on the κ-carrageenan-based films. **Figures 4(c)**, **(e)**, and **(f)** present the TSP/carrageenan-based polymer blend films of different ratios (TSP20, TSP60, and TSP80). In this composition of polymer blend, the aggregate structure seems to be presented. This might be due to the incompatibility between two different polysaccharides. This observation has been explained in the study by Xie et al. [24], which explains that TSP molecules could easily aggregate because of the reduced galactose and could also lead to hydrophobic interactions. **Figure 4(d)** shows the reduction of the

congested structure on the film's surface for TSP40, indicating the improved compatibility between TSP and carrageenan at this ratio. However, visible clumps were also spotted, which might be due to the incomplete dissolution of the carrageenan particles.

The surface of the pure pectin film appeared uniformly smooth, as per illustrated in **Figure 5(a)**. A study by Baghi et al. [25] also clarifies that the surface of pure pectin film is smooth. When pectin and carrageenan were blended, the textured surface of carrageenan was reduced, as shown in **Figures 5(c)** and **(d)** for PE20 and PE40, respectively. Meanwhile, the disappearance of textured surface and the formation of smoother and homogenous ones were observed for PE60 and PE80, as shown in **Figures 5(e)** and **(f)**, respectively. A homogeneous and smooth surface structure is generally preferable for films since it can help to increase mechanical strength, barrier qualities, and overall efficient use [26]. Although PE60 and PE80 appeared smoother, their brittleness limits their practicality, while PE40 remained flexible.

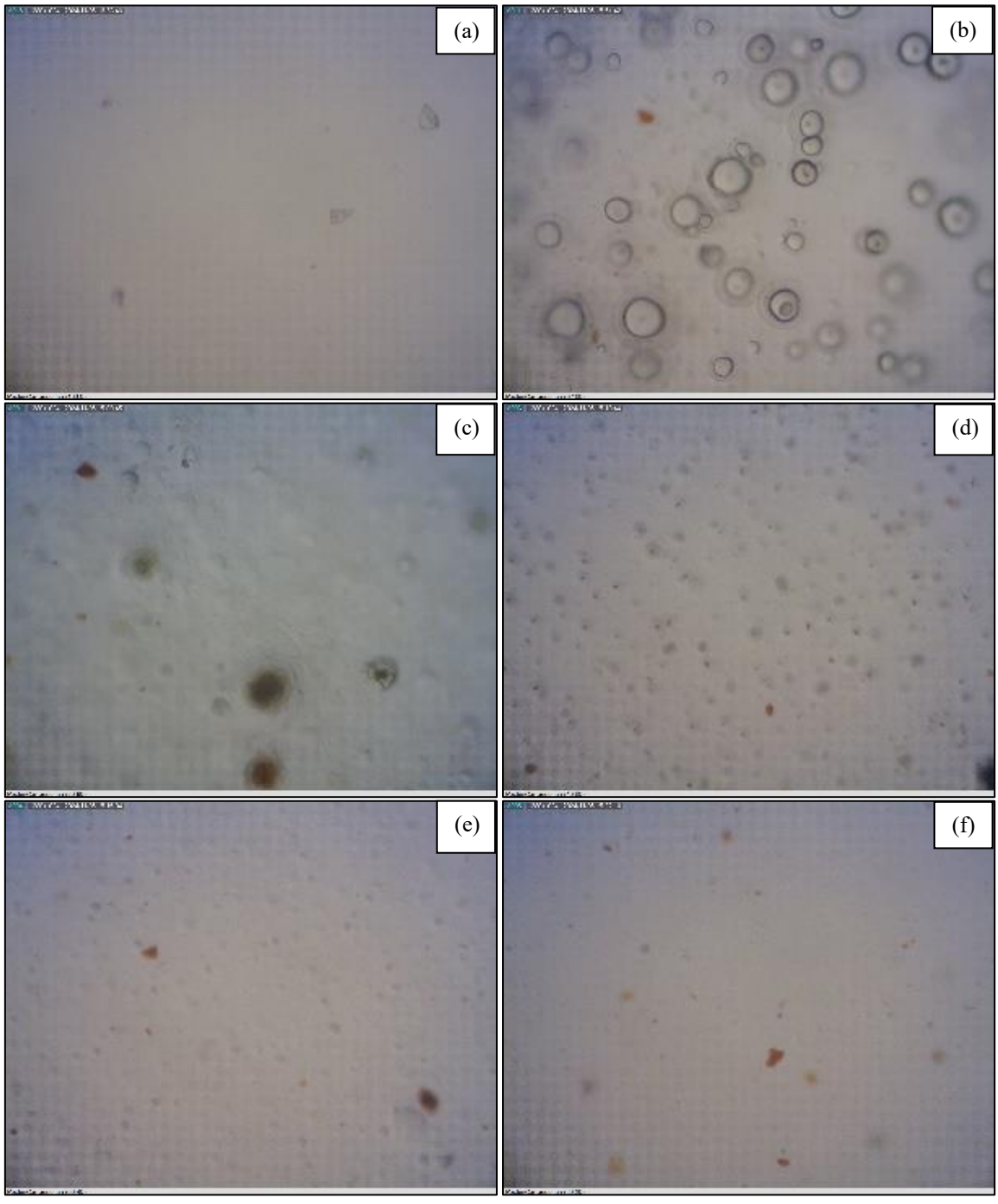

Figure 5. Optical micrographs for (a) pure pectin, (b) pure carrageenan, (c) PE20, (d) PE40, (e) PE60, and (f) PE80.

Table 4. Thickness of films.

Sample films	Thickness (mm)
Pure TSP	0.1877 ± 0.036
TSP20	0.1757 ± 0.021
TSP40	0.1217 ± 0.002
TSP60	0.1310 ± 0.007
TSP80	0.1306 ± 0.007
Pure Pectin	0.1260 ± 0.008
PE40	0.1070 ± 0.003

Mechanical Studies of Polymer Blend Films

The mechanical strength of the polymer blend films was assessed through tensile testing. **Table 4** lists the thickness of all the samples. The thickness of pure TSP and pectin were 0.1877 ± 0.036 mm and 0.1260 ± 0.008 mm, respectively. Meanwhile, after being blended with carrageenan, the thickness of all the polymer blend films was observed to decrease. This is probably due to the reduction of hydrogen bonding which leads to a more compact structure as reported by Murthy [27].

Figure 6 shows the plots of tensile strain and Young's Modulus against pure TSP and TSP/ carrageenan polymer blend electrolyte films of different compositions (TSP20, TSP40, TSP60, and TSP80). The tensile strength of pure carrageenan was reported by Rahman et al. [28] at the value of 77.83 ± 1.18 MPa, with the elongation at the break value of 10.23 ± 1.02%. As for the TSP-CMC blend film's tensile strength, Ji et al. [29] reported the value of 13.60 ± 0.09 MPa. The tensile strain of pure TSP was 2.2276 %. When TSP was blended with carrageenan, the tensile strain increased up to 4.3223% for the 40:60 ratio film, indicating the improvement in the flexibility of the film. This might be due to the interaction between TSP and carrageenan (as confirmed from the FTIR analysis), which hinders the formation of hydrogen bonding between individual polymer chains. However, when TSP and carrageenan was blended at the ratios of 60:40 (TSP60) and 80:20 (TSP80), the tensile strain decreased. This is because of the presence of aggregate structure due to the incompatibility of TSP and carrageenan at these ratios, as confirmed by morphological analyses. The tensile strain for TSP40 showed the highest result compared to other TSP/carrageenan compositions, indicating the synergistic effect of the polymers at that ratio.

Young's Modulus is a measure of the stiffness of a material and the value exhibits the opposite trend to tensile strain. The Young's Modulus value for TSP was 3372.7867 MPa. The highest modulus of pure TSP indicates the rigidity of the film because of its strong hydrogen bonding and semi-crystalline structure, which prevent deformation. The value decreased to 2059.3050 MPa and 2478.3575 MPa for TSP20 and TSP40, respectively, indicating the reduced stiffness of the materials. This may result from the improvement of the amorphous phase of the material after the polymer blend was mixed at the ideal ratio, due to the TSP-carrageenan interaction which prevents the formation of hydrogen bonding between individual polymer chains. This is in line with the study by Zainuddin et al. [21], which reported that the combination of CMC and KC may result in more amorphous areas and fewer opportunities for individual molecules to recrystallize. The Young's Modulus value for TSP60 increased to 3275.7121 MPa, with reduced flexibility, and decreased to 2814.1200 MPa for TSP80, with improved flexibility.

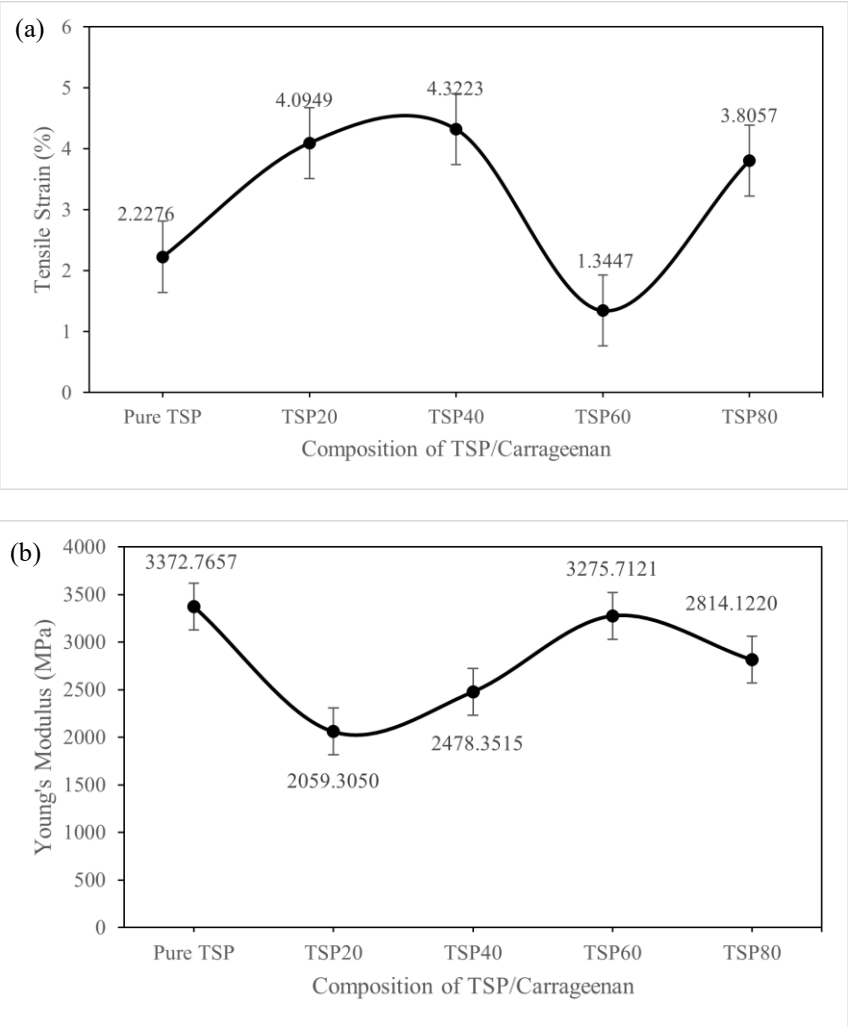

Figure 6. Mechanical properties of TSP/carrageenan blend electrolytes films, (a) tensile strain and (b) Young's Modulus.

The plots for tensile strain and tensile stress against sample composition for pure pectin and PE40 are shown in **Figure 7**. The tensile strain for PE40 was 0.7833%, which is higher than pure pectin at 0.5557% (**Figure 7(a)**). This indicates improved flexibility of the polymer blend of pectin/carrageenan 40:60 (PE40) compared to pure pectin. This can be attributed to the interaction between pectin and carrageenan, which hinders the creation of hydrogen bonds, thereby yielding a flexible film. The pectin-carrageenan interaction can be further confirmed via FTIR analysis. This observation suggests that the combination of pectin and carrageenan at the ratio of 40:60 provides synergistic effects, hence enhancing the elasticity of the film.

The tensile stress result for PE40 was 16.7389 MPa, which is lower than pure pectin at 21.3163 MPa (**Figure 7(b)**). The tensile stress of pure pectin film has been reported at 16.94 $\pm$ 0.59 MPa by Bello and Peresin [30]. As tensile stress is lower, flexibility is higher. The decrease in tensile stress indicates the decrease in resistance to deformation. This is because there are less intermolecular crosslinks within the pectin molecules in the films [31].

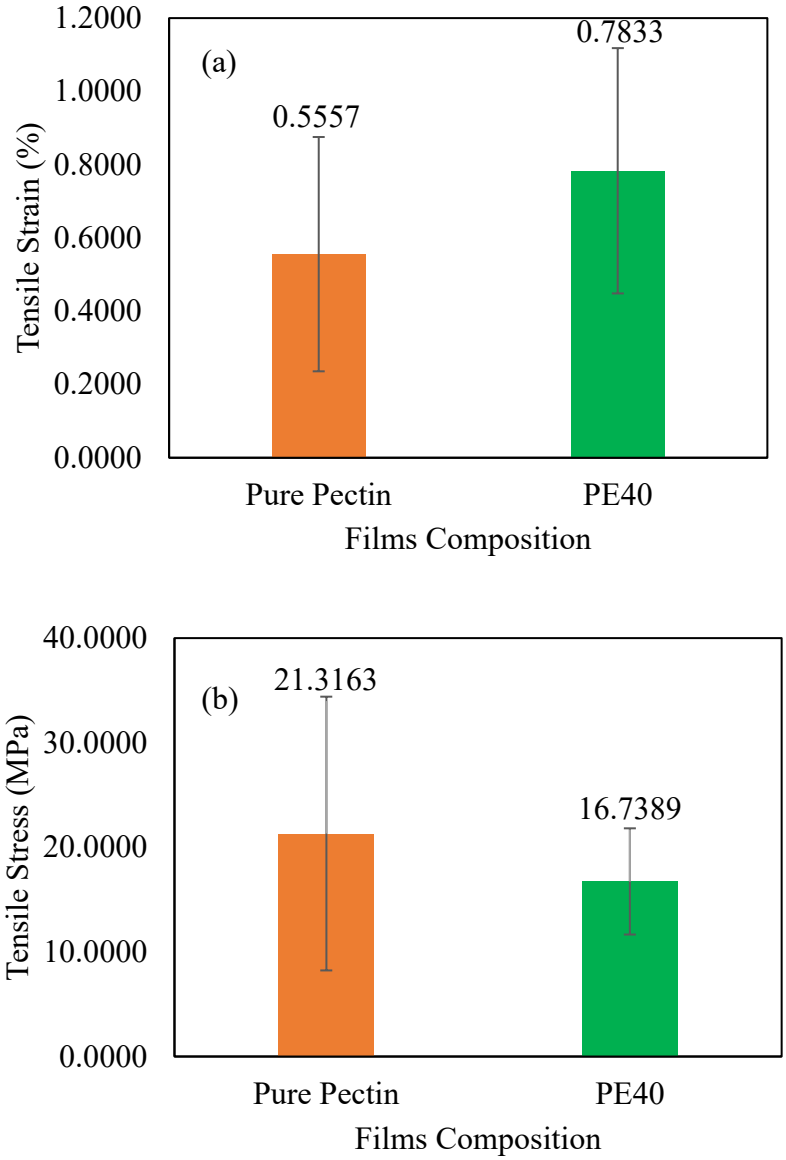

Figure 7. Mechanical properties of pectin/carrageenan polymer blend films, (a) tensile strain and (b) tensile stress.

Electrical Studies of Polymer Blend Films

Figure 8 presents the Cole-Cole plots for pure TSP, pure pectin, TSP40, and PE40. In the high frequency region, a half semicircle was observed for pure TSP, while depressed semicircles were observed for pure pectin, TSP40, and PE40. Meanwhile, in the low frequency region, spikes were observed for TSP40 and PE40. According to Elakkiya et al. [32], semi-circle and spike represent the bulk resistance (R_b) and the charge transfer resistance and capacitance of the electric double layer formed at the electrolyte/electrode interfaces, respectively. Therefore, the TSP40 and PE40 samples can be represented as a resistance-capacitance (RC) circuit, as shown in **Figure 9**. However, due to observed deviations of the impedance spectra from ideal behavior, the capacitors (C) were substituted with constant phase elements (CPEs).

From the Cole-Cole plot, the R_b value was obtained, and the ionic conductivity was calculated using Equation (1). **Table 5** lists the ionic conductivity values for all the samples.

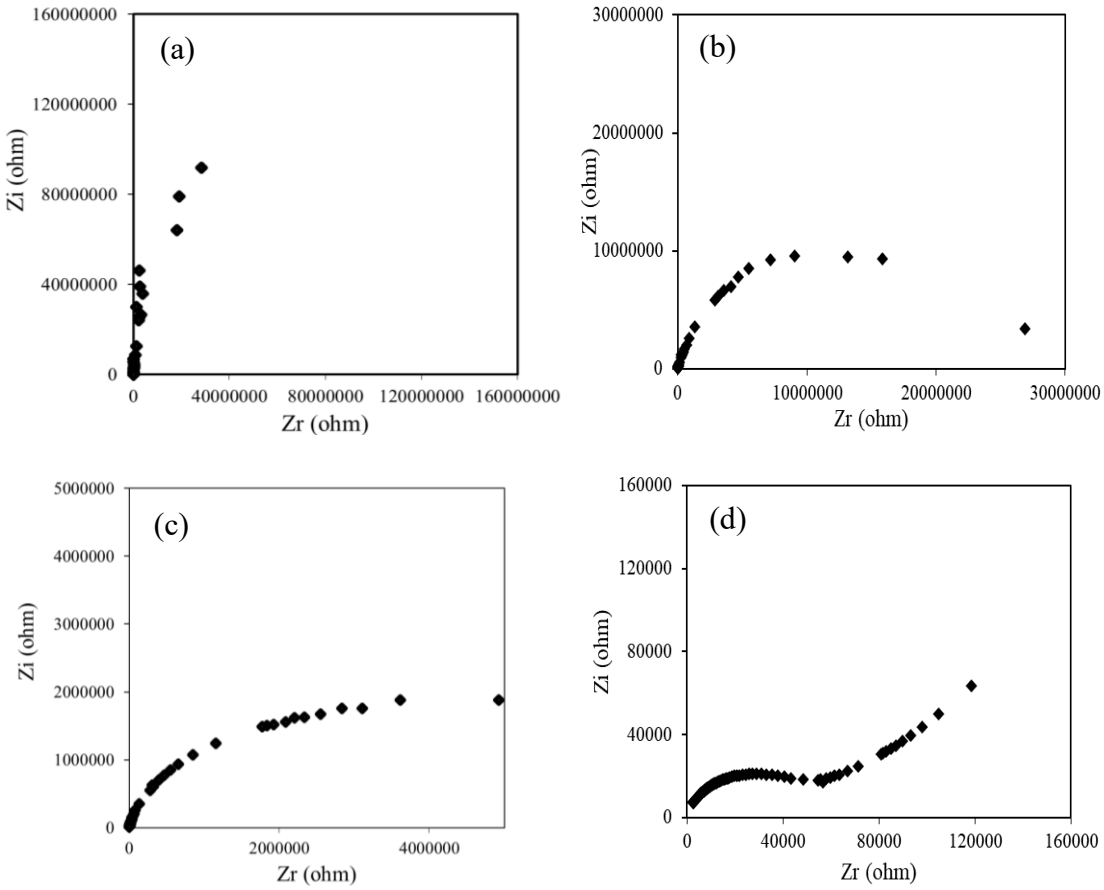

Figure 8. Cole-Cole plots for (a) pure TSP, (b) pure pectin, (c) TSP40, and (d) PE40.

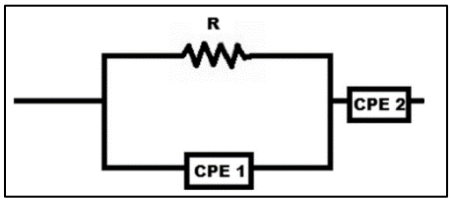

Figure 9. The equivalent circuit for TSP40 and PE40.

Table 5. Ionic conductivity for pure TSP, pure pectin, TSP40, and PE40.

Sample Composition	Ionic Conductivity, σ (S cm^{-1})
Pure TSP	$3.48 \pm 0.11 \times 10^{-10}$
Pure Pectin	$6.38 \pm 5.03 \times 10^{-10}$
TSP40	$1.78 \pm 1.23 \times 10^{-08}$
PE40	$6.58 \pm 6.38 \times 10^{-07}$

As listed in **Table 5**, the pure TSP and pure pectin films exhibited the ionic conductivity of $3.48 \pm 0.11 \times 10^{-10}$ S cm^{-1} and 6.38×10^{-10} S cm^{-1}, respectively. The ionic conductivity then increased to $1.78 \pm 1.23 \times 10^{-8}$ S cm^{-1} and $6.58 \pm 6.38 \times 10^{-7}$ S cm^{-1} when TSP (TSP40) and pectin (PE40), respectively, were blended with carrageenan at the composition of 40:60. The improvement in the flexibility of the films, as confirmed from the tensile test, also can contribute to the improvement in ionic

conductivity as a flexible film will provide good adhesions between the electrolyte and electrode. This is consistent with the finding by Zainuddin et al. [21], which indicates that the increasing composition of kappa-carrageenan could result in the increasing ionic conductivity of the polymer blend of CMC/kappa-carrageenan. The research by Jansi et al. [10] also reported that the ionic conductivity for pectin and sodium alginate at a composition of 40:60 was 1.26×10^{-7} S cm^{-1} at room temperature. PE40 was observed with the highest ionic conductivity, while pure pectin was the lowest. Thus, this indicates that the addition of carrageenan to pectin enhances ionic conductivity. In conclusion, as PE40 shows the improvement in term of flexibility and ionic conductivity, it is expected that the ions can move freely in it. Thus, to provide conducting species, the PE40 film was doped with 15 wt% of LiTf for further characterization.

Formation of LiTf-doped Pectin/Carrageenan Polymer Blend Films

The LiTf-doped pectin/carrageenan film at the composition of 40:60 (PE40+LiTf) was successfully prepared, as shown in **Figure 10(b)**; while **Figure 10(a)** displays the control sample. The flexible and free-standing film was observed after 15 wt% of LiTf was doped to the PE40 film. The film was then analyzed further using FTIR, OM, and EIS.

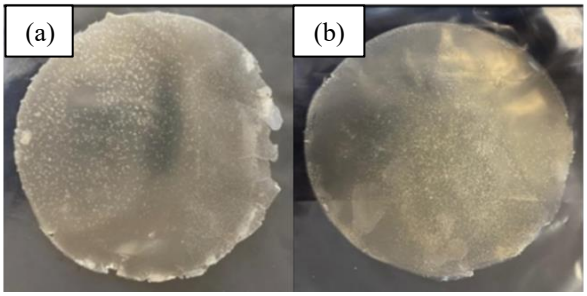

Figure 10. Films of (a) PE40 and (b) PE40+LiTf.

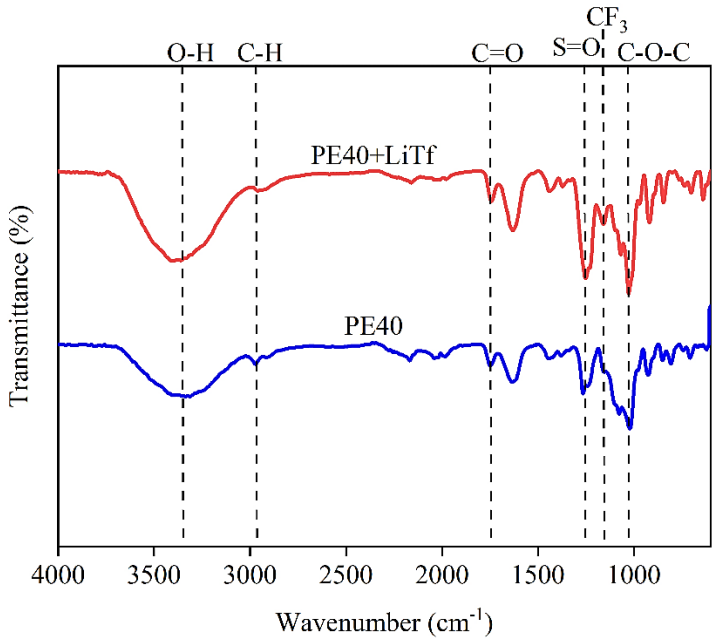

Figure 11. FTIR spectra of PE40 and PE40+LiTf.

Table 6. Peak assignments and shifts in the vibrational peaks of PE40 and PE40+LiTf.

Peak Assignment	Wavenumber (cm^{-1})		References
	PE40	PE40+LiTf	
O-H stretching	3327	3394	[10]
C-H stretching	2971	2954	[34]
C=O stretching	1744	1747	[35]
SO_3 stretching	1257	1251	[16]
CF_3 stretching	-	1157	[16]
C-O-C stretching	1013	1027	[20]

Structural Studies of LiTf-doped Pectin/ Carrageenan Polymer Blend Films

The FTIR spectra for PE40 and PE40+LiTf are depicted in **Figure 11**, while the wavenumbers of all peaks are listed in **Table 6**. The peaks for PE40 appeared at 3327, 2971, 1744, 1257, and 1013 cm^{-1}, representing O–H stretching, C–H stretching, C=O stretching, S=O stretching, and C–O–C stretching, respectively. For PE40+LiTf, the new peak representing the salt was observed at 1157 cm^{-1} (CF_3 stretching) indicating successful incorporation of LiTf into the polymer blend system. Also, after the addition of 15 wt% LiTf, the O–H stretching, C=O stretching, and C–O–C stretching peaks shifted to 3394, 1747, and 1027 cm^{-1}, respectively. These observations indicate that interactions had occurred between Li^+ ions of LiTf with oxygen atoms in the pectin/carrageenan blend, as also confirmed in a study by Perumal et al. [33] which studied pectin and $LiClO_4$ salt. The increase in the peak intensity of S=O stretching, representing the sulfate group of carrageenan, was also observed, indicating the interaction between the sulfate group and the Li^+ ions from the salt.

Electrical Studies of LiTf-doped Pectin/Carrageenan Polymer Blend Films

Figure 12 depicts the Cole-cole plots for PE40 and PE40+LiTf. Both samples showed a depressed semicircle and a spike. According to Jansi et al. [10], the resistance to charge transfer at the interaction between the electrodes is represented by a semicircle at the start of the plot, whereas diffusion-controlled processes are indicated by a spike, which shows the migration of the ions toward the electrode.

R_b was determined from the Cole-Cole plots by intercepting the semicircle with the Zr axis [32]. After that, the ionic conductivity was computed using Equation (1). The ionic conductivity values for both samples are listed in **Table 7**.

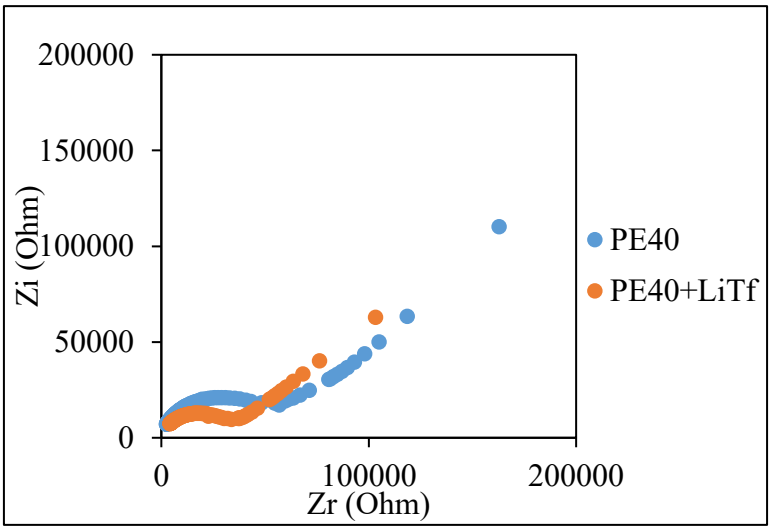

Figure 12. Cole-cole plots for PE40 and PE40+LiTf.

Table 7. Ionic conductivity for PE40 and PE40+LiTf.

Sample Composition	Ionic Conductivity, σ (S cm^{-1})
PE40	$6.58 \pm 6.38 \times 10^{-7}$
PE40+LiTf	$2.95 \pm 1.71 \times 10^{-6}$

The ionic conductivity of PE40+LiTf was recorded as 2.95 10^{-6} S cm^{-1} when 15 wt% of LiTf was doped. Thus, the addition of 15 wt% of LiTf increased one order of magnitude if compared to PE40. This is probably due to the presence of the conducting species consisting of Li^+ and $CF_3SO_3^-$ ions. Apart from that, the optimum ratio of pectin/carrageenan in the PE40 sample also acts as a good polymer host by providing the amorphous structure and more possible coordinating sites which ease the mobility of Li^+ ions. This observation can be further supported by a study done by Perumal et al. [36], which found that the amorphous nature of the material improves inter- and intra-chain mobility, as well as Li^+ ion transport, resulting in high ionic conductivity. A study by Shilpa and Saratha [35] found that during complexation, the blend film's amorphicity may rise, which could lead to an increase in ionic conductivity. The ionic conductivity obtained in our investigation (~10^{-6} S cm^{-1}) is comparable with that of other polymer electrolyte systems as shown in **Table 8,** making it promising for application in energy storage devices. However, it is significant that the ionic conductivity is somewhat greater in comparison to the study by Marf et al. [37], which used polyvinyl alcohol/chitosan (50:50) with 40 wt% NH_4I in their polymer electrolyte system.

Table 8. List of ionic conductivity for polymer blend electrolyte systems.

Sample Composition	Ionic Conductivity, σ (S cm^{-1})	References
Pectin/Carrageenan (40:60) + 15 wt% LiTf	2.05×10^{-6}	This study
Polyvinyl Alcohol/Chitosan (50:50) + 40 wt% NH_4I	9.10×10^{-7}	[37]
Polyvinyl Alcohol/Chitosan (50:50) + 20 wt% $LiClO_4$	3.00×10^{-6}	[14]
Chitosan/Polyethylene Glycol (70:30) + 2 wt% $LiClO_4$	8.70×10^{-6}	[13]
Chitosan/Methylcelullose (75:25) + 40 wt% LiI	6.26×10^{-6}	[38]
Sodium Alginate/PVA (60:40) + 10 wt% NaI	$4.27 \pm 0.09 \times 10^{-6}$	[39]

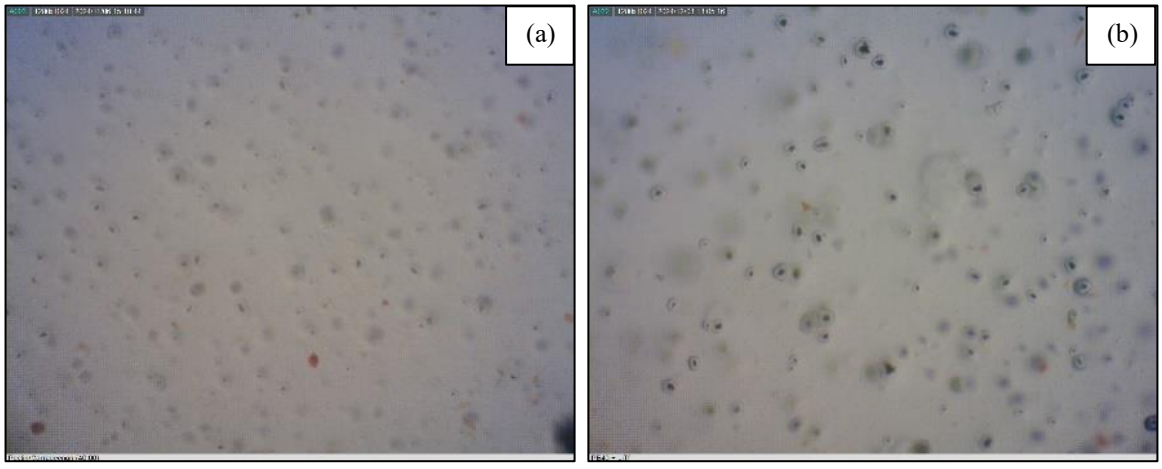

Figure 13. Optical micrographs of (a) PE40 and (b) PE40+LiTf.

Morphological Studies of LiTf-doped Pectin/ Carrageenan Polymer Blend Films

Surface investigation can reveal the material's structure and electrical characteristics [40]. The 10x magnification optical micrographs of PE40 and PE40+LiTf are displayed in **Figure 13**. The surface has a small particle texture, pores, and grey spots, as shown in **Figure 13(b)**. According to Khellouf et al. [41], the creation of pores may boost ionic conductivity by creating new ion routes, with morphological changes caused by the interaction of dissociated ions with the polymer blend. This can be linked by the observation in the FTIR analysis in **Figure 10**.

CONCLUSION

In this study, flexible, free-standing, with the improvement in ionic conductivity, TSP/carrageenan (TSP40) and pectin/carrageenan (PE40) blend films were successfully prepared at a composition of 40:60, hence proving the synergistic effect of the polymer blends at this ratio. The increase in tensile strain further confirms the improvement in term of the flexibility of the polymer blend films. This is attributed to the TSP-carrageenan and pectin-carrageenan interactions, as confirmed by FTIR analyses, which prevent the formation of hydrogen bonding within the individual polymer chains. Additionally, the improved flexibility of the polymer blend film also contributes to the increment in the ionic conductivity values, due to the improved electrode-electrolyte contact. The morphology of TSP40 and PE40 also improved due to the reduction of textured surface and the formation of smooth film. For future work, XRD and DSC analyses along with fatigue and bending tests are suggested to further corroborate these findings. When 15 wt% of LiTf was incorporated into the pectin/carrageenan blend system, the ionic conductivity increased to one order of magnitude from 6.58×10^{-7} S cm^{-1} to 2.95×10^{-6} S cm^{-1}. The enhancement of the ionic conductivity is due to the presence of the conducting species from LiTf. Also, more possible coordinating sites and amorphous phase of the blend system at the optimum ratio contribute to the easy movement of Li^+ ions. In addition, the presence of pores was also observed from the optical micrograph of PE40+LiTf, indicating the creation of new ion routes as the result of the polymer-salt interaction. Hence, the PE40+LiTf exhibited improved ionic conductivity (~10^{-6} S cm^{-1}) and stable morphology, making it a promising solid polymer electrolyte for solid-state lithium-ion batteries. To strengthen the practical relevance of the optimum sample, future work should include its fabrication with electrode materials and subsequent analysis through Linear Sweep Voltammetry (LSV), transference number measurements, charge-discharge tests, and thermogravimetric analysis (TGA).

ACKNOWLEDGEMENTS

The authors are very grateful to the Faculty of Applied Sciences, UiTM Perlis branch for giving the full support for this research. Thanks also goes to FRGS, grant FRGS/1/2023/STG05/UITM/02/19, for the financial support given.

REFERENCES

1. Chattopadhyay, J., Pathak, T. S. & Santos, D. M. F. (2023) Applications of polymer electrolytes in lithium-ion batteries: A review. *Polymers*, **15(19)**, 3907.

2. Rayung, M., Aung, M. M., Azhar, S. C., Abdullah, L. C., Su'ait, M. S., Ahmad, A. & Jamil, S. N. A. M. (2020) Bio-based polymer electrolytes for electrochemical devices: Insight into the ionic conductivity performance. *Materials*, **13(4)**, 838.

3. Obuebite, A. A., Gbonhinbor, J. R., Onyekonwu, M. & Akaranta, O. (2021) Comparative analysis of synthetic and natural polymer for enhanced oil recovery. *International Journal of Science and Engineering Investigations*, **10(113)**, 14–19.

4. Song, L., Sun, S. & Zhao, X. (2023) Ethylene carbonate plasticized polymer electrolyte for chloride ion batteries with enhanced reversible capacity. *Solid State Ionics*, **399**, 116314.

5. Huang, P. -C., & Chou, W. -C. (2023) Unveiling the hidden dangers of plasticizers: A call for immediate action. *Toxics*, **11(6)**, 527.

6. Qadeer, A., Kirsten, K. L., Ajmal, Z., Jiang, X. & Zhao, X. (2022) Alternative plasticizers as emerging global environmental and health threat: Another regrettable substitution? *Environmental Science & Technology*, **56(3)**, 1482–1488.

7. Zare, Y. (2016) Study of nanoparticles aggregation/ agglomeration in polymer particulate nano-composites by mechanical properties. *Composites Part A: Applied Science and Manufacturing*, **84**, 158–164.

8. Blatt, M. P. & Hallinan, D. T. (2021) Polymer blend electrolytes for batteries and beyond. *Industrial & Engineering Chemistry Research*, **60(48)**, 17303–17327.

9. Grira, S., Alkhedher, M., Abu Khalifeh, H. & Ramadan, M. (2024) Recent advancements in utilizing biomass materials for aqueous electrolytes in rechargeable batteries. *Renewable and Sustainable Energy Reviews*, **206**, 114867.

10. Jansi, R., Vinay, B., Revathy, M. S., Sasikumar, P., Marasamy, L., Janani, A., Haldhar, R., Kim,

S. -C., Almarhoon, Z. M. & Hossain, M. K. (2024) Synergistic blends of sodium alginate and pectin biopolymer hosts as conducting electrolytes for electrochemical applications. *ACS Omega*, **9(12)**, 13906–13916.

11. Perumal, P., Abhilash, K., Sivaraj, P. & Selvin, P. C. (2019) Study on Mg-ion conducting solid biopolymer electrolytes based on tamarind seed polysaccharide for magnesium ion batteries. *Materials Research Bulletin*, **118**, 110490.

12. Habep, N. A. (2023) The effect of nanoalumina (Al_2O_3) filler on the structural, morphological and electrical properties of poly(methyl methacrylate) (PMMA) / 50% epoxidized natural rubber (ENR 50) electrolytes [Bachelor's thesis, Universiti Teknologi MARA]. *EPrints*.

13. Sudhakar, Y. N., Selvakumar, M. & Bhat, D. K. (2012) $LiClO_4$- doped plasticized chitosan and poly(ethylene glycol) blend as biodegradable polymer electrolyte for supercapacitors. *Ionics*, **19(2)**, 277–285.

14. Rathod, S. G., Bhajantri, R. F., Ravindrachary, V., Pujari, P. K. & Sheela, T. (2014) Ionic conductivity, and dielectric studies of LiClO4 doped poly(vinylalcohol)(PVA)/chitosan(CS) composites. *Journal of Advanced Dielectrics*, **04(04)**, 1450033.

15. Butler, I. P., Banta, R. A., Tyuftin, A. A., Holmes, J., Pathania, S. & Kerry, J. (2023) Pectin as a biopolymer source for packaging films using a circular economy approach: Origins, extraction, structure and films properties. *Food Packaging and Shelf Life*, **40**, 101224.

16. Fauzee, M. M. H., Suddin, N. F. A., Muhd Zailani, N. A., Nazir, K., Syed Ismail, S. N., Mohd Zaini, N. A., & Yahya, S. (2024) Impact of choline chloride/1,4-butanediol deep eutectic solvent on tamarind seed polysaccharide-based polymer electrolyte. *Malaysian Journal of Chemistry*, **26(4)**, 167-177.

17. Said, N. S., Olawuyi, I. F. & Lee, W. Y. (2024) Tailoring pectin-PLA bilayer film for optimal properties as a food pouch material. *Polymers*, **16(5)**, 712.

18. Serra, J. P., Salado, M., Correia, D. M., Gonçalves, R., Del Campo, F. J., Lanceros-Mendez, S. & Costa, C. M. (2023) High-Performance sustainable electrochromic devices based on carrageenan solid polymer electrolytes with ionic liquid. *ACS Applied Engineering Materials*, **1(5)**, 1416–1425.

19. Alshammari, O. A. O., Alhar, M. S. O., Al-Otaibi, A., AlRashidi, A. A., Alshammari, A. F., Alzahrani, E. A., Elsayed, N. H., Monier, M. & Youssef, I. (2025) Synthesis of photo-responsive κ-carrageenan-based hydrogels for drug delivery application. *International Journal of Biological Macromolecules*, **289**, 138797.

20. Halim, N., Muhd Zailani, N., Nazir, K., Ismail, S. & Latif, F. (2024) Effect of lithium triflate (LiTf) salt on the properties of the pectin-based polymer electrolytes films. *Scientific Research Journal*, **21(1)**, 145–162.

21. Zainuddin, N. K., Saadiah, M. A., Majeed, A. P. P. A. & Samsudin, A. S. (2018) Characterization on conduction properties of carboxymethyl cellulose/kappa carrageenan blend-based polymer electrolyte system. *International Journal of Polymer Analysis and Characterization*, **23(4)**, 321–330.

22. Liu, R., Chi, W., Jin, H., Li, J. & Wang, L. (2022) Fabricating κ-carrageenan/carboxymethyl cellulose films encapsulating bromothymol blue fixed rice straw fiber for monitoring meat freshness. *Industrial Crops and Products*, **187**, 115420.

23. Sudhakar, M. P., Venkatnarayanan, S. & Dharani, G. (2022) Fabrication and characterization of bio-nanocomposite films using κ-carrageenan and Kappaphycus alvarezii seaweed for multiple industrial applications. *International Journal of Biological Macromolecules*, **219**, 138–149.

24. Xie, F., Zhang, H., Nie, C., Zhao, T., Xia, Y. & Ai, L. (2021) Structural characteristics of tamarind seed polysaccharides treated by high-pressure homogenization and their effects on physico-chemical properties of corn starch. *Carbohydrate Polymers*, **262**.

25. Baghi, F., Ghnimi, S., Agusti, G., Dumas, E. & Gharsallaoui, A. (2024) Development and characterization of pectin-based antimicrobial packaging films containing nanoemulsified trans-cinnamaldehyde. *Applied Sciences*, **14(6)**, 2256.

26. Qiang, T., Ren, W. & Chen, L. (2023) Biodegradable, high mechanical strength, and eco-friendly pectin-based plastic film. *Food Hydrocolloids*, **149**, 109539.

27. Murthy, N. S. (2006) Hydrogen bonding, mobility, and structural transitions in aliphatic polyamides. *Journal of Polymer Science Part B Polymer Physics*, **44(13)**, 1763–1782.

28. Rahman, S., Konwar, A., Konwar, A. N., Dubey, S., Ghosh, M. P., Boro, B., Thakur, D. & Chowdhury, D. (2024) AG Nanoparticle Incorporated Guar Gum–Sodium Alginate–I-Carrageenan Tribiopolymer Blended Cloth Waste Lint Extracted Cellulose Nanocrystal Anti-

microbial Composite Film. *Biomacromolecules*, **25(3)**, 1491–1508.

29. Ji, S., Sun, R., Wang, W. & Xia, Q. (2023) Preparation, characterization, and evaluation of tamarind seed polysaccharide-carboxymethylcellulose buccal films loaded with soybean peptides-chitosan nanoparticles. *Food Hydrocolloids*, **141**, 108684.

30. Bello, F. & Peresin, M. S. (2024) Multifunctional pectin and lignin-containing cellulose nanofiber films with improved UV resistance and mechanical properties. *Food Hydrocolloids*, **157**, 110378.

31. Pereira, D. G. M., Vieira, J. M., Vicente, A. A. & Cruz, R. M. S. (2021) Development and characterization of pectin films with salicornia ramosissima: biodegradation in soil and seawater. *Polymers*, **13(16)**, 2632.

32. Elakkiya, M., Revathy, M. S., Jansi, R., Janani, V. A., Kumar, A., Agrawal, A., Mishra, V. K., Shaaban, I. A. & Hossain, M. K. (2025) Investigation on structural and electrical properties of sodium alginate/PVP solid blend polymer electrolyte. *Materials Today Communications*, **42**, 111067.

33. Perumal, P., Christopher Selvin, P., Selvasekarapandian, S., Sivaraj, P., Abhilash, K. P., Moniha, V. & Manjula Devi, R. (2019) Plasticizer incorporated, novel eco-friendly biopolymer based solid bio-membrane for electrochemical clean energy applications. *Polymer Degradation and Stability*, **159**, 43–53.

34. Priyadarshi, R., Kim, S. -M. & Rhim, J. -W. (2021) Pectin/pullulan blend films for food packaging: Effect of blending ratio. *Food Chemistry*, **347**, 129022.

35. Shilpa, R. & Saratha, R. (2020) Biodegradable pectin- guar gum blend electrolyte for solid state lithium ion batteries. *AIP Conference Proceedings*, **2270(1)**, 100006.

36. Perumal, P., Christopher Selvin, P., Selvasekarapandian, S. & Sivaraj, P. (2019) Structural and electrical properties of biopolymer pectin with $LiClO_4$ solid electrolytes for lithium ion polymer batteries. *Materials Today: Proceedings*, **8**, 196–202.

37. Marf, A. S., Abdullah, R. M. & Aziz, S. B. (2020) Structural, morphological, electrical, and electrochemical properties of PVA: CS-based proton-conducting polymer blend electrolytes. *Membranes*, **10(4)**, 71.

38. Abdullah, O. G., Hanna, R. R., Ahmed, H. T., Mohamad, A. H., Saleem, S. A. & Saeed, M. A. (2021) Conductivity and dielectric properties of lithium-ion biopolymer blend electrolyte based film. *Results in Physics*, **24**, 104135.

39. Cyriac, V., Ismayil, Mishra, K., Sudhakar, Y. N., Rojudi, Z. E., Masti, S. P. & Noor, I. M. (2024) Suitability of NaI-complexed sodium alginate–polyvinyl alcohol biodegradable polymer blend electrolytes for electrochemical device applications: Insights into dielectric relaxations and scaling studies. *Solid State Ionics*, **411**, 116578.

40. Adam, A. A., Soleimani, H., Shukur, M. F. B. Abd., Dennis, J. O., Hassan, Y. M., Abdulkadir, B. A., Yusuf, J. Y., Ahmed, O. S. S., Salehan, S. S., Ayub, S. & Abdullahi, S. S. (2024) Novel composite polymer electrolytes based on methylcellulose-pectin blend complexed with potassium phosphate and ethylene carbonate. *Biomass Conversion and Biorefinery*, **14(10)**, 11665–11682.

41. Khellouf, R. A., Durpekova, S., Cyriac, V., Cisar, J., Bubulinca, C., Lengalova, A., Skoda, D. & Sedlarík, V. (2023) Correlations between the dopant concentration and ion transport properties of plasticized NaCMC-pectin polyblend electrolyte membranes for electrochemical device applications. *Solid State Ionics*, **402**, 116379.